CAAP Quarterly Report

Date of Report: July 10th 2019

Prepared for: *U.S. DOT Pipeline and Hazardous Materials Safety Administration*

Contract Number: 693JK31850008CAAP

Project Title: Fluorescent Chemical Sensor Array for Detecting and Locating Pipeline Internal Corrosive Environment

Prepared by: Dr. Ying Huang (NDSU) and Dr. Hao Wang (Rutgers University)

Contact Information: Dr. Ying Huang, Email: ying.huang@ndsu.edu, Phone: 701.231.7651

For quarterly period ending: July 7th 2019

Business and Activity Section

(a) Contract Activity

Discussion about contract modifications or proposed modifications

None.

Discussion about materials purchased

None. Purchases for experiments will be in next quarter.

(b) Status Update of Past Quarter Activities

In this quarter, the university research team worked on Task 2.2 of the above mentioned project, including literature review on the simulation tools for numerical analysis on the survivability of possible installation of the polymer based sensors inside the pipeline with high pressure and fast moving liquids and experimental preparation on testing the survivability of possible sensors under passing of a cleaning pig (Task 2.2), in addition to an outreach program to Native American high school students to expand the educational impact of this project. *In Quarterly Report #2 (Q2), Task 2.1 was planned to be performed in this quarter (Q3), however, in the beginning of this quarter, the graduate student (Wei Xu, Ph. D. student) in Chemistry Department at NDSU decided to quit his graduate study. Thus, although the potential applicable polymers have been selected, there was no graduate student available to perform the planned Q3 Future Work Item #1, and without testing results in Q3 Future Work Item #1, Q3 Future Work Item #2 also cannot be conducted as scheduled. However, we are fortunate to recruit another new graduate student who will start working on Task 2.1 of this project in late July. Therefore, the Q3 Future Work Item #1 and #2 will remain as future work for Q4 and we will report the finding of Task 2.1 in next quarter (Q4). This change has been further explained in student mentor section. Since we were ahead of schedule for Q2 in the chemical sensor development, this change of student assignment is not expected to induce any delay in the overall project schedule.*

(c) Cost share activity

Tuition Waiver for two graduate students (6 credits per student, $693.68 per credit) ended up with $8,324 of cost share in this quarter).

(d) Task 2 Development of Fluorescent/Colorimetric Chemical Sensor Array for Internal Corrosive Water Detection

1. Background and Objectives in the 3rd Quarter

1.1 Background

This project is designed to develop passive colorimetric/fluorescent chemical sensor array for locating and detecting corrosive water inside pipes. Inside the pipelines, the transported crude oil may include a hot mixture of free water, carbon dioxide (CO_2), hydrogen sulfide (H_2S) and microorganisms. The different chemical components inside oil/water environment such as HCO_3^- / CO_3^{2-}, Fe^{3+}, S^{2-}, H^+ or pH may result in different internal corrosion mechanisms, such as sweet corrosion or sour corrosion. The passive colorimetric sensor array to be developed in this project is intended to detect the concentration changes of the five above mentioned important chemical species in the internal oil/water environment of the pipeline and use these detected environmental data to predict the internal corrosion progressing of pipelines.

1.2 Objectives in the 3rd Quarter

In this quarter, the research team started to 1) model the pipeline with fluid to test whether the developed sensor can survive the harsh service condition inside the pipeline (Task 2.2, subtask: test the survivability of the developed sensor array in oil/water environment and optimize the sensor dimension); 2) prepare the experiments to test the survivability under operational and cleaning stage inside a pipe (Task 2.2, subtask: test the survivability of the developed sensor array); and 3) Outreach to Native American high school students.

2. Results and Discussions

2.1 Test the Survivability of the Developed Sensor Array in Oil/Water Environment and Optimize the Sensor Dimension (Task 2.2)

In last quarter, we simulated the potential impact of a cleaning pig on the sensor without consideration of flow inside the pipe. However, to test the practical survivability of the developed sensor array in oil/water environments and optimize the sensor dimension, numerical simulation of flow is required. There are various tools or commercial software existing to perform the modeling of a fluids in a pipe such as GAMBIT, FLUENT, and ANASYS Computational Fluid Dynamics (CFD). To Search for an appropriate simulation tool, in this quarter, the research team conducted literature review on the existing tools to simulate the movement and pressure of fluids in a pipeline. Due to the fact that the sensor array needs not only survive in an operational fluid condition but also during impacts such as water hammer, the literature review included two parts: 1) numerical simulation of normal flow in a pipe; and 2) simulation of fluid impact (water hammer) in a pipe. *These reviews will serve as the basis to develop the customized model for calculating the induced shear stress from the fluids that may be experienced by the polymer-based chemical sensors to be attached in the pipe wall, which determines their survivability and dimension required.*

2.1.1 Numerical Simulation of Normal Flow in a Pipe

To test the survivability of the sensor array in an operational flow inside a pipe, numerical simulation of normal flow in a pipe is needed. The simulation of regular oil or water flow in pipelines is of interest in

many engineering applications. In the case of oil as fluid, Haitao and Frank (2016) applied the k-epsilon turbulent model in GAMBIT and FLUENT to determine the oil/water volume fraction distribution and wall shear stress in pipelines. They found that if the oil fluid flows at low velocities in horizontal pipes, the upward part immediately passing the elbow in the upward inclined pipes and both the straight and the downward parts of the downward inclined pipes are the likely area for corrosion. The maximum wall shear stress was observed at the top of the elbow and the bottom of the upper part in upward inclined pipes and the bottom of the elbow and the upper part in downward inclined pipes. Alias (2014) used RNG k-ε turbulent model and grid independent study in FLUENT to simulate oil-water two-phase flow in a horizontal pipe, which derived that as the flow velocity increases, the pressure gradient also increases. Fairuzov (2000) performed simulations of a two-fluid pipeline model to investigate the behavior of oil-water flow during transients caused by changes in the water volume fraction at the entrance to the pipeline. An increase in the water flow rate results in the formation of a shock but the smoothening of the water holdup waterfront occurs when the water volume fraction decreases. Anand et al. (2014) applied FLUENT to perform analysis on flow characteristics of stratified wavy, stratified mixed, and annular flow through the horizontal pipeline. It was found that in the annular flow, the total pressure of the mixture decreases with increase in oil velocity. Oil volume fraction reaches its maximum point at the center in core annular flow, but at the upper side in stratified flow.

In the case of slurry (solid-liquid) as transmitting flow, Kaushal (2012) used Mixture and Eulerian two-phase model in FLUENT to model the mono-dispersed fine particles at high concentration. The Mixture model fails to predict pressure drops correctly compared with experimental data and the number of error increases rapidly with the slurry concentration. Fairly accurate predictions were from Eulerian model for pressure drop at all the efflux concentrations and flow velocities except near the pipe bottom. Chen (2009) applied Eulerian multiphase approach based on the kinetic theory of granular flow with the RNG k-$\sum$ turbulent model to simulate the coal-water slurries (CWS) in horizontal pipelines. Slurry flow characteristics, such as constituent particle, concentration distribution, and velocity distribution as well as pressure gradients were seen in the results. Gravity difference between large and small particles and strong particle-particle interaction mainly affect the concentration distribution and velocity distribution. Ekambara (2009) investigated the effect of different parameters in slurry and results indicated that the particles are asymmetrically distributed in the vertical plane and the degree of asymmetry increases with particle size increasing (2009).

For gas-liquid pipeline, Ghorai (2006) used Eulerian-Eulerian model in FLUENT to model the two-phase gas-liquid flow in pipes and investigated the influence of various variables on flow behavior such as gas velocity, the volume fraction of liquid and interfacial roughness. The flow field characteristics and a correlation of (f_i/f_w) in wavy stratified flow regime were obtained. Also, Abdolkarimi (2013) modeled a 90° bended gas pipeline using ANASYS CFD based on the Lagrangian framework and found that as a radial component of gas velocity through the bend increases, the larger particles move toward the outer wall of the bend and this area is more likely to corrode.

In addition, simulations of bubbly flow in pipelines attract attention to discover the flow regime. The internal phase distribution of co-current, air-water bubbly flow in a horizontal pipeline using the volume averaged multiphase flow equations with two different models (k–ε with constant bubble size and with population balance model) made a good quantitative agreement with the experimental data. It was found that increasing the gas flow rate with fixed liquid flow rate would increase the local volume fraction. The maximum volume fraction locates near the upper pipe wall and the profiles tend to flatten with liquid flow rate increasing (Ekambara 2008). Taha (2006) used FLUENT to investigate the motion of single Taylor bubbles in vertical tubes and a description of the bubble propagation in both stagnant and flowing liquids

was got from results. Multiphase flow models for the description of mono- and polydisperse bubbly flows in the Eulerian framework with inhomogeneous MUSIG model using ANSYS CFX were presented by Frank et al (2008). The models took drag and non-drag interphase momentum transfer into account. The mono- and polydisperse bubbly flows models were thoroughly validated and compared to experiments results.

The movement of fluid would also generate heat. Heat transfer in the pipes was also studied by ANASYS CFD simulation to find the influence factors for the movement of fluid. Jayakumar et al. (2010) studied the variation of local Nusselt number along the length and circumference at the wall of a helical pipe and movement of fluid particles in a helical pipe by CFD simulations with various coil parameters. Correlations for prediction of Nusselt number as a function of the angular location of the point was presented. Ahmadvand et al. (2010) studied heat transfer and fluid flow characteristics of swirling flows generated by axial vanes and found that heat transfer enhancement is strongly dependent on blade angle (or inlet swirl intensity) and the Re number has no significant influence and swirl deforms velocity distributions. Along axial direction, flow accelerates close to the wall and tends to reverse at the central region and tangential velocity component is divided into two distinct regions semi-central forced and annular free vortex.

Based on these literature reviews, potentially, FLUENT or ANASYS CFD can be used as candidates to model and test the survivability of the sensor array in oil/water environments when the sensors are installed inside an oil/gas pipeline during a regular operational condition.

2.1.2 Numerical Simulation of Fluid Impact (Water Hammer)

The sensor array not only is required to be operational during normal flow inside pipelines, but also survive the flow before, during, and after a water impact, such as water hammer. Water hammer exists when flows suddenly stop during valve closure, pump start and stop, fluids with different flow rates suddenly meet, fluid flow velocity in the tube suddenly changes, etc. (Muhlbaure 2004).

Theoretical Solution: To understand water hammer, here we explain the theoretical derivation for how water hammer induces. Kinetic energy is transferred to potential energy and pressure waves are formed by the increment of the internal pressure (Streeter 1998; Thorley 2004) and based on different continuity and momentum equations, the fluid impact of water hammer could be presented as:

$$\mathrm{v}\frac{\partial H}{\partial s} + \frac{\partial H}{\partial t} + v\sin\theta + \frac{a^2}{g}\frac{\partial v}{\partial s} = 0 \tag{1}$$

$$g\frac{\partial H}{\partial s} + \frac{\partial v}{\partial t} + v\frac{\partial v}{\partial s} + \frac{\lambda v|v|}{2D} = 0 \tag{2}$$

where, H is water head height, g is the gravity, v is water velocity, D is internal diameter of the pipeline, a is the velocity of pressure wave, θ is the angle between the pipe axis and the horizontal line, λ is resistance coefficient, and t is the thickness of pipeline. The traditional equation of impact pressure is

$$\Delta\mathrm{p} = a\rho\Delta\mathrm{v} \tag{3}$$

where, $\Delta\mathrm{p}$ is the impact pressure, $\Delta\mathrm{v}$ is the velocity change of fluid, ρ is relative density, and a is the velocity of the pressure wave, which is calculated using the equation below.

$$a = \frac{\sqrt{\frac{K}{\rho}}}{\sqrt{1+\frac{KD}{Et}}} \tag{4}$$

where, K is bulk modulus, E is Young's modulus, and C is the constraint coefficient of the pipeline (Allievi 1925).

Joukowski et al. (1904) proposed the use of arithmetic to calculate transient flow, which ignores friction and lays the foundation for transient flow analysis. A correction factor C is added to the equation, which equals to one for the pipe system in which the expansion joint is set. If the pipeline imposes a strong constraint along the path, it is taken as $1-\nu^2$, where ν is the Poisson ratio (Wylie 1984; Wylie 1993). Filion et al. (2002) proposed a graphical method that ignores friction in theoretical derivation but is corrected by other methods. Based on complete 3D continuity equation and Navier-Stokes equations, Ghidaoui (2001) derived quasi-two-dimensional equations using an ensemble averaging process in which the assumptions inherent in the quasi-two-dimensional equations are made explicit.

Numerical Simulations: Based on the above-mentioned theory, there are several simulation tools which can be used to simulate water hammer effects including method of characteristic (MOC), wave characteristic method (WCM), implicit method, and finite element method such as CFD. Ghidaoui and Kolyshkin (2001) applied MOC method to study the laminar and turbulent water hammer flows and got the base flow velocity profiles and found that Reynolds number and a dimensionless time scale are the main parameters that govern the stability of transient flows. Ghidaoui et al. (2002) used WCM to compare two turbulence water hammer models, namely the two-layer and the five-layer eddy viscosity and evaluated the accuracy of their quasi-steady and axisymmetric assumptions and both models are in good agreement, confirming that the turbulence modeling of water hammer flows is insensitive to the magnitude and distribution of the eddy viscosity within the pipe core. Zhao (2004) formulated first- and second-order explicit finite volume methods of Godunov-type for water hammer problems, compared its performances with MOC and found they are in good agreement. Wood (2005) and Wood et al. (2005) investigated MOC and WCM to analyze the transient flow in water distribution networks including pipe friction and they have the same modeling accuracy. In addition, they showed that the number of calculations per time step required by WCM does not increase when more accuracy is required. WCM would be time efficient for analyzing large pipe networks. Saikia and Sarma (2006) presented a numerical model using MOC and Barr's explicit friction factor for simulation of the water hammer problems and made an examination for rapid valve closure in downstream of a long conduit with a reservoir upstream.

Developments in computational modeling have also promoted the use of computational fluid dynamics (CFD) for modeling the fluid (Dargahi 2006). Nikpour et al. (2014) used experimental and numerical simulation methods to study the water hammer phenomenon in the water supply network, compared the experimental data with the results of computational fluid dynamics (CFD) and found that CFD can be successfully used in the modeling and simulation of water hammer phenomena. Wu et al. (2010) adopted the CFD method to analyze the transient characteristics of the pump during the rapid opening process of the discharge valve and then compared the obtained result with the test data.

However, CFD is not able to do some simulations due to the limitation of computation power, such as the entire primary loop. Thus, coupled methods can be used. The 1D and 3D MOC-CFD coupled approach to study the interaction water hammer and pump during the rapid closing of the valve and found the analysis based on MOC-CFD coupled method is closer to the actual situation when compared with that using MOC alone because fluid inertia is taken into consideration (Wu 2015). Ruprecht and Helmrich (2003) used coupled 1D MOC and 3D CFD to investigate the system oscillations of a water power plant caused by the draft tube flow. *Therefore, based these literature review, CFD combined with MOC would be potentially a good candidate to model the water hammer effect on the sensor array when attached inside the pipe.*

In next quarter, we will start to model the flow in pipeline and their impact on the sensor array using FLUENT and CFD whichever results in the best findings on the sensors' performance. Sensitivity and sensor characterization will be simulated to determine the appropriate sizes of sensors in normal and water hammer impacts.

2.2 P*repare the Experiments to Test the Survivability under Operational and Cleaning Stage inside a Pipe* (Task 2.2)

In the last quarter, a FEM was established to get the simulation result of the friction and internal stress of sensors under scratching action by sealing discs from pipeline inspection gauges. This quarter also started to prepare the experimental study on the feasibility of the sensor under the operational flow and under the passing of a cleaning pig which is part of Task 2.2. The experiments were expected to validate the sensor survivability in a near-practice condition for more reliable application prospect. *Literature review of PIG motions in pipelines to avoid any risk of failures which others may have taken and based on the literature review the most applicable experiment design are proposed for a potential success of testing in the current work.*

2.2.1 literature Review on Experimental Design:

Numbers of researchers (Solghar et al 2012, Esmaeilzadeh et al 2009, and Nieckele et al 2001) have established numerical models of PIG motions in the pipeline and some of them conducted experiments to study the stress in pipeline portions as well as the gauges under inspection movements. Zhang et.al (2015) conducted numerical and experimental research of friction and dynamic characteristics of sealing disc passing through girth weld in pipelines. This study conducted experimental validation tests as illustrated in Figure 1 to evaluate the real friction and dynamic response of the seal disc. In this setup, an 8 in. steel pipe about a meter in length with prefabricated girth weld was used. The height of the girth weld is as 3 mm above the internal surface of pipe and the length of the girth weld is 8 mm above the internal surface of pipe. The pipe was fixed on the ground by use of supports. Inner diameter of the pipe was 203 mm. An 8-in. bi-directional PIG was connected to a hydraulic cylinder (Nonfe Hydraulic Equipment CO., LTD., Peking, China) with 30 kN thrust force, which was controlled by a hydraulic control circuit. The PIG was fixed to a short rigid shaft connected to a piston rod. The PIG was forced along the pipe at a constant speed using the hydraulic cylinder. The propulsion force can be regarded as a frictional force between the sealing disc and the pipe when the PIG has a steady motion. The propulsion force of PIG was measured using a force sensor (model CFBLCS2; SinoMeasure Instrument Technology CO., Ltd., Hangzhou, China) linked to data acquisition system. The data acquisition system consists of a NI data acquisition card (NI USB-6343) connected to a laptop and power supply, with a custom VI written in LabView for recording the data. Parameters for three different sealing discs labeled as A, B and C are listed in Table 1.

Before the start of the experiment, the PIG was placed within the pipe. A single piece of sealing disc was installed on the front and rear sides of the PIG. The force sensor was mounted on the piston rod connected to the PIG. After setting up all the equipment, the hydraulic cylinder was started, which moved the PIG with the single sealing disc along the smooth segment of the pipe. The hydraulic cylinder was turned down after the front sealing disc passed through the girth weld. The speed of the piston rod in each experiment was kept constant at 20 mm/s. During this process, propulsion force was digitally acquired and recorded for analysis.

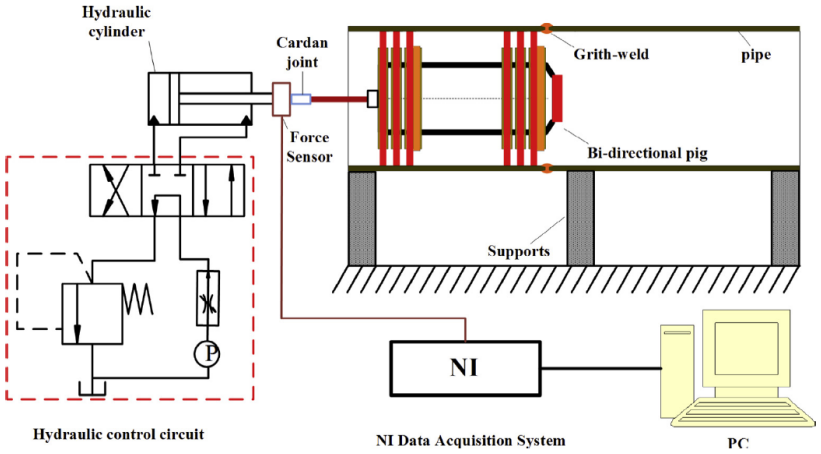

Figure 1 Schematic diagram of the experiment setup (Zhang et.al 2015)

Table 1 Sealing disc configurations used for testing

ID	*Outer Diameter of the sealing disc (mm)*	*Thickness of the sealing disc (mm)*	*Comments*
A	203	10	Normal/thin
B	203	15	Normal/thick
C	206	15	Large/thick

During this experiment, the propulsion force F_t of the hydraulic cylinder was measured as a function of time as the sealing disc passed through the girth weld. The measured forces are shown in Figure 2. The green, red and purple curves represent the propulsion force acting on the sealing discs A, B and C, respectively. The dotted black line indicates the time when the sealing disc comes into contact with the girth weld. The sudden drop seen for the three curves occurs as the sealing disc completely passes over the girth weld. As shown in Figure 2, the sealing disc A, B and C come in contact with the girth weld at the same time. A rise in the propulsion force was observed immediately after contact with the girth weld. After the propulsion force reaches a maximum, a sudden and rapid drop in force was observed. Based upon these experimental results, the process as the single sealing disc passing through the girth weld can be divided into three distinct stages: (1) start-up stage, (2) climbing stage, and (3) slope stage.

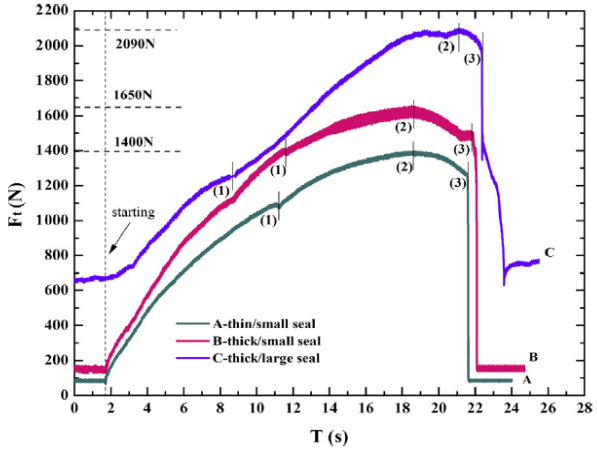

Figure 2 Changing trends of propulsion force with time (Zhang et.al 2015)

For simulation, a 2D axisymmetric finite element model was modeled in this study (Zhang et.al 2015) as shown in Figure 3. The model was solved using Abaqus 6.10 (Dassault Systèmes, France). The FE model consisted of a pipe with the girth weld, a sealing disc and two clamp plates. Clamp plates were used to fix the sealing discs into proper position. The pipe was fixed on the ground. The whole body (clamp plates and sealing disc) was moved with a specified displacement. Two displacement- loading sequences are considered in two separate analysis steps. The first analysis step considers axial displacement of the clamp plate. In the next analysis step, loading is also an axial displacement of the same clamp plate.

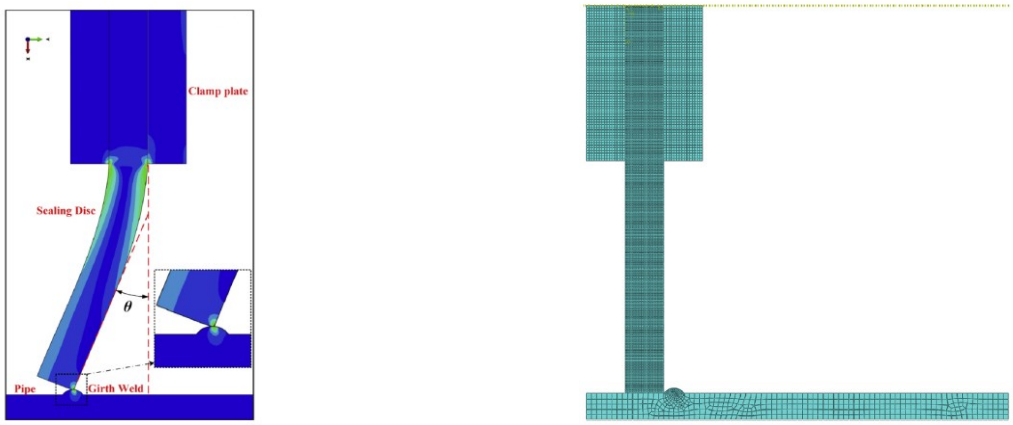

(a) (b)

Figure 3 2D axisymmetric finite element model (Zhang et.al 2015)

The sequence of steps occurring as the sealing disc passing through the girth weld in pipeline during the FEM simulation was shown as in Figure 4. According to the FEM results, the process of the sealing disc model passing through the girth weld model can also be sub-divided into three stages which are consistent with the experimental results: (1) start-up stage, (2) climbing stage, and (3) slope stage. The results indicated that as time in the start-up stage increases, both the bending angle and contact stress increased sharply up to a certain maximum value.

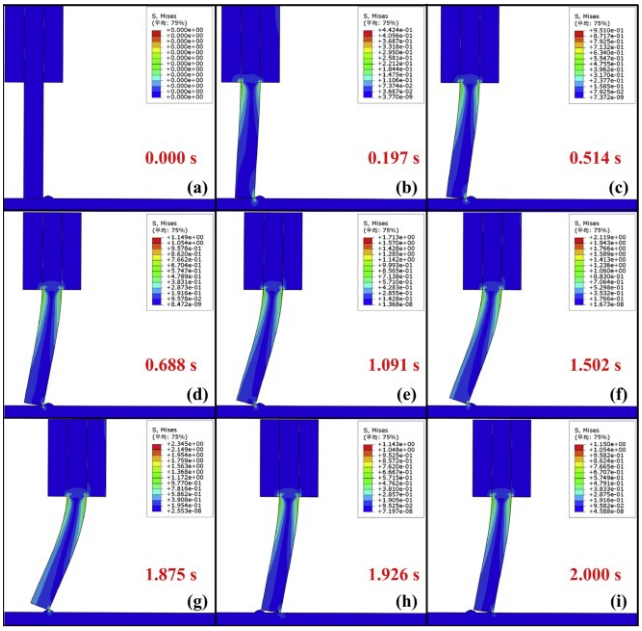

Figure 4 The process of the sealing disc passing through the girth weld in pipeline simulated using FEM.

The contact stress increased from 0 MPa to 0.82 MPa, as shown in Figure 5a and the bending angle increased from 0° to 11°, as shown in Figure 5b. In order to reduce the friction, the sealing disc would bend

to change the contact coupling from surface contact to line contact. The radial outer end of sealing disc clings to the starting point of the girth weld model in the start-up stage. Whereas, the radial inner ends of sealing disc with clamp plates kept moving along the X-axis. The bending angle and the contact stress continue to increase. The total time of the start-up stage was 0.68 s. The radial inner end of the sealing disc gradually moved away from start-up stage and began to climb the weld model. During this process, as the height of the weld model increased, the bending angle of sealing disc continued to increase, but the growth slowed down. The contact stress increased from 0.82 MPa to 1.65 MPa, as shown in Figure 5a and the bending angle increased from 11° to 23°, as shown in Figure 5b. In this stage, the friction force changed from static to kinetic friction. The displacement along X-axis increased from 0 to 1.8 mm, and the displacement along Y-axis increased linearly from 0 to 3.8 mm. The total time of the climbing stage was about 1.14 s. During the sloping stage, there was a minor increase in contact stress from 1.68 MPa to 1.70 MPa, as shown in Figure 5c, but was not enough to cause sealing disc to bend further. The displacement along X-axis increased from 1.8 mm to 2 mm, and the displacement of Y-axis increased from 3.8 mm to 4 mm. The total time of the sloping stage was about 0.06 s.

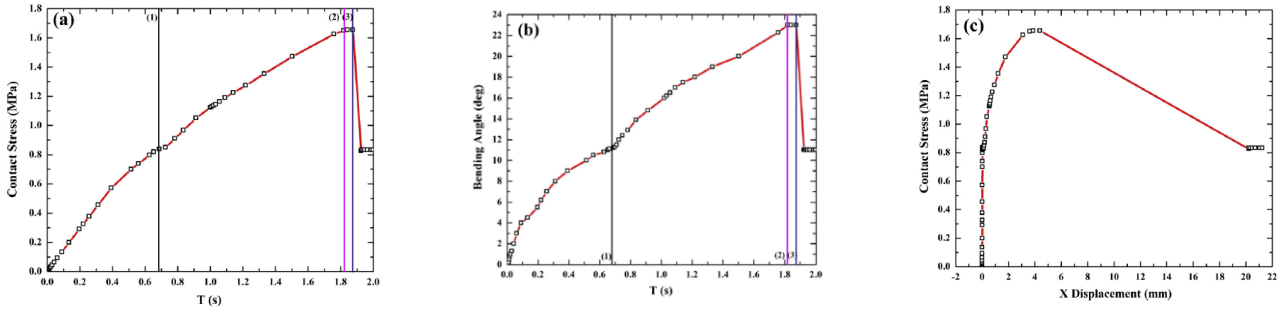

(a) (b) (c)

Figure 5 (a) Contact stress between sealing disc and girth weld. (b) Bending angle of sealing disc during the process that the sealing disc model passes through the girth weld. (c) Contact stress between sealing disc and girth weld as a function of X displacement (Zhang et.al 2015)

Zhu et.al (2014, 2015a, 2015b) developed experimental and 2D numerical analysis to study the pig contact force in a gas pipeline. The torque experiment setup of bypass-valve in speed control pig is shown in Figure 6. In order to get enough bypassing time, four air reservoirs connected in series are used to storage high-pressure gas. Two air compressors were used to compress the air into the air reservoirs. Pressure sensors were used to collect the pressures at the rear of the pig, at the front and rear of bypass-valve and the pressure in the air reservoir. A torque sensor was used to collect the load torque of the inner valve. Data Acquisition Unit is designed to display and store the dates.

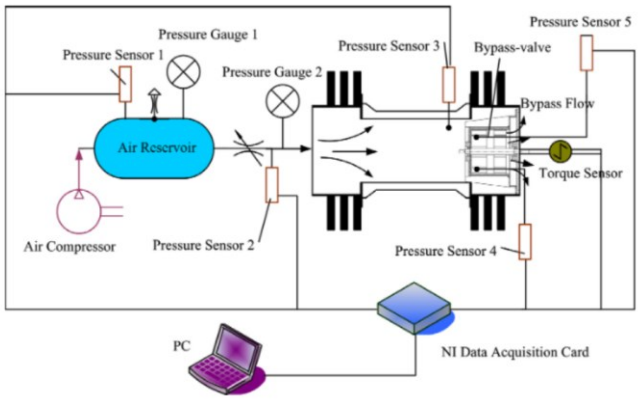

Figure 6 Schematic diagram of the experiment (Zhu et.al 2014)

The prototype can be seen in Figure 7a. In this experiment, five pressure sensors were needed. The pressure sensors with serial numbers from 1 to 5 were mounted at the top of the air reservoir, the rear of the pig, the rear of the bypass valve, and the front of the bypass-valve respectively. The torque sensor and pressure sensors were all linked to the Data Acquisition Unit. Data Acquisition consists of NI data acquisition card, laptop, and electric power. As it is shown in Figure 7b, before the experiment, the body of the pig was fixed on the ground and the outer valve was fixed on the body of the pig. The inner valve was connected to a torque sensor which consists of a weighing sensor and a supporting arm. The supporting arm fixed on the central axis of the inner valve was used to transmit the torque to compressive force, which can be measured by the weighing sensor. During the measurement, a preload was applied to the weighing sensor. If the inner valve rotates the effect of bypass fluid, the preload will increase or decrease depending on the direction of rotation.

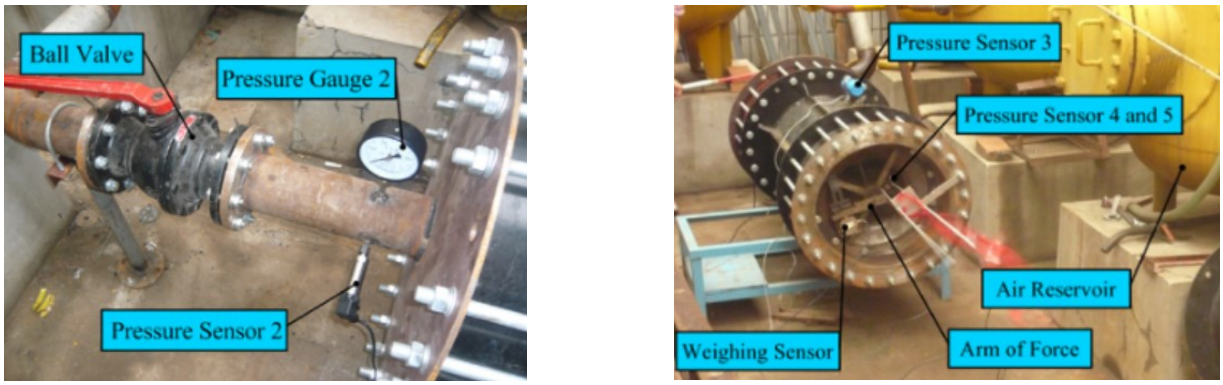

(a) (b)

Figure 7 Prototype of the experiment (Zhu et.al 2014)

After this experiment, the changing trends of load torque, differential pressure over the pig and air reservoir pressure with time at the opening of 0.387°, 1.549°,5°and 10°are shown in Figure 8. The change time from 0 to24 sec was chosen, as the trends were not obvious when it was over 24 sec. We can see from these four typical figures when the ball valve was opened, the pressure in air reservoir was declined quickly. At the same time, the differential pressure over the bypass-valve had a sudden increase and then declined with the air reservoir pressure. The trend of the load torque was similar to the differential pressure over the bypass-valve. Another point is, when the opening increased, the differential pressure over the bypass-valve and the load torque acting on it fluctuated more seriously, as it is shown in Figure 8.

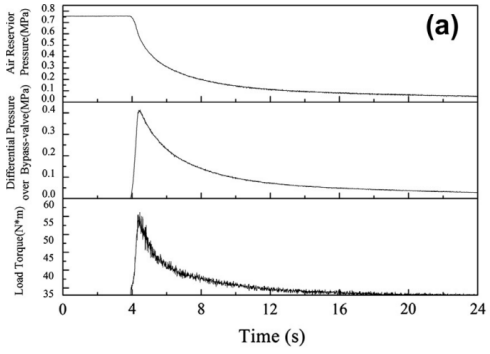

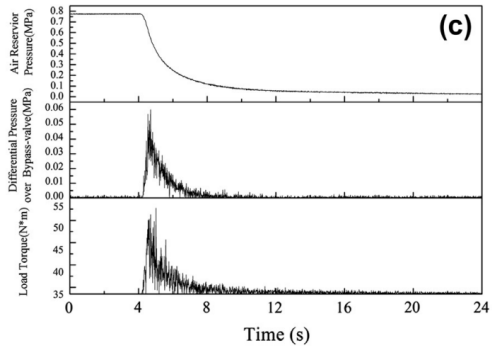

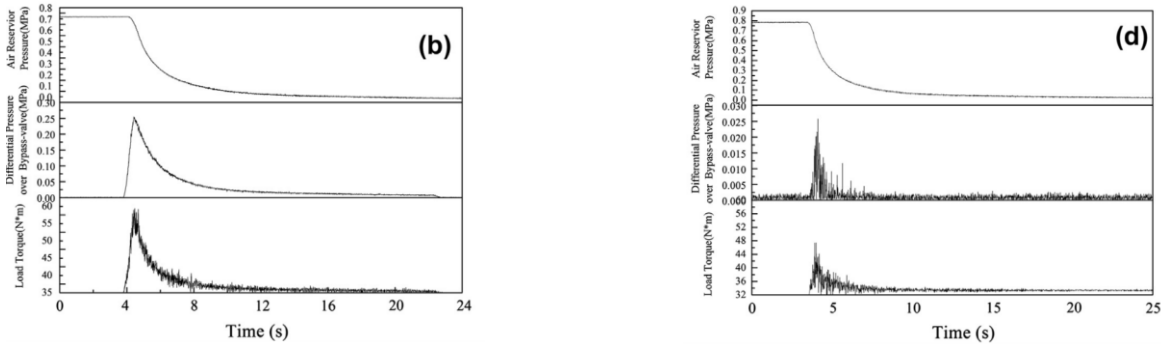

Figure 8 The changing trends of load torque, differential pressure over the pig and air reservoir pressure with time at the opening of (a) 0.387°, (b) 1.549°, (c) 5° and (d) 10° (Zhu et.al 2015a, 2015b)

2.2.2 Experiment Design in this Project

Based on the literature review, to validate the simulated result of the sensor survivability in pipelines, a lab experiment was designed in this quarter to simulate the real process of a sealing rubber disk on PIG passing through the steel pipeline as shown in Figure 9 which illustrates the PIG motion in a pipeline. In the FEM as shown in Figure 10a, a partial section of sealing disk and pipeline was presented because of the axisymmetry.

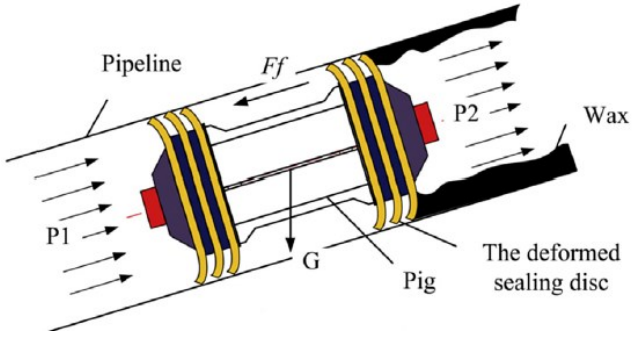

Figure 9 Pipeline inspection process

Figure 10b and 10c show the experimental design following the instructions from the literature review (Zhang et.al 2015 and Zhu et.al 2014, 2015a, 2015b) as detailed in last section. A sensor will be attached in the inside surface of the a steel pipe with a diameter of 8 in. or 12 in steel pipe, a rubber disk will be welded onto a clamp plate which will be clamped on a MTS loading machine to provide the simulated movement of the rubber disk as a cleaning pig. The MTS Loading machine (Figure 11) in NDSU CIE 108 was chosen as loading platform because of the capability of returning the load curve, which illustrates the force of top loading jig to measure the friction coefficient.

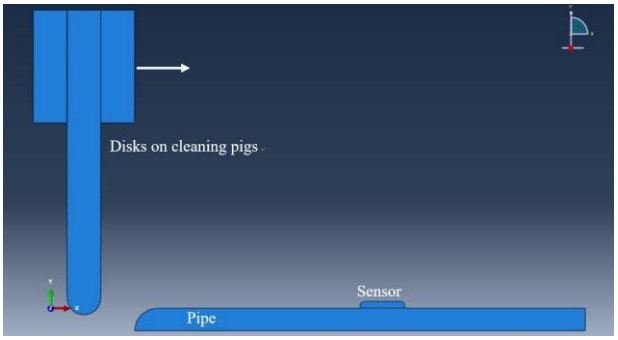

(a) FEM sketch

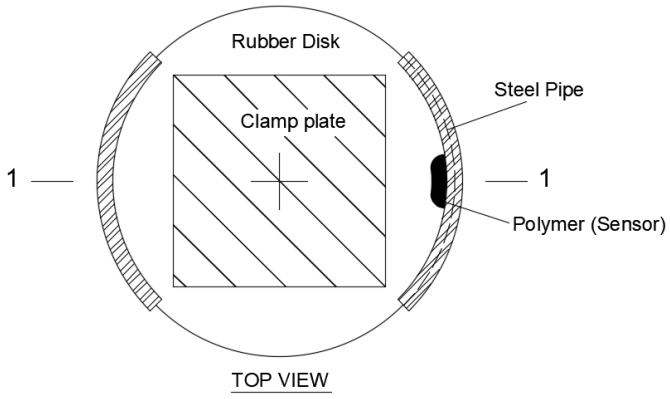

(b) Top view

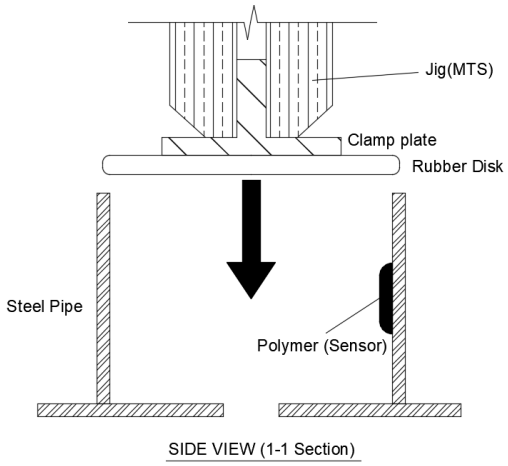

(c) Side view

Figure 10 Experimental design

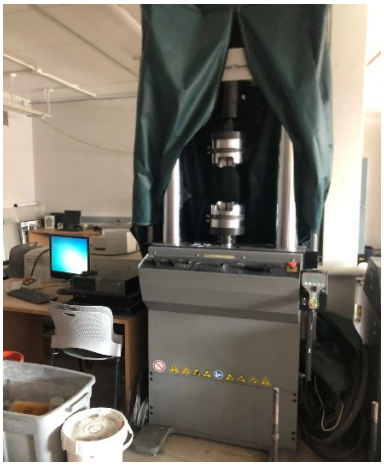

Figure 11 MST machine

In the simulation, the thickness of sensor is divided into 10 levels (from 1 to 10mm). Thus, for the experiment design, replaceable epoxy follows the same dimension plan. To execute the designed experiments, below are details for purchase plan to get the experiments set up as designed:

a) Sealing disk-Polyurethane rubber: Each of the company can fabricate customized urethane products, and by now, FallLine and Unicastinc seem to be the most satisfying provider because of the availability of small devices and reasonable price. The quoted price will come up later based on the submitted 3D-design.

Table 2 Sealing disk provider

Company	Tel	Website
FallLine	800-325-5463	https://www.fallline.com/
Unicastinc	800-503-9569	https://www.unicastinc.com
Blaylock	817-717-4097	http://www.blaylock-gasket.com
Smooth-On	800-762-0744	https://www.smooth-on.com/category/urethane-rubber/
Reynoldsam	888-904-1999	https://www.reynoldsam.com/product-category/urethane-rubber/

b) Steel pipe: Based on Normal Pipe Size, DN-150 (Table 3) and DN-250 (Table 4) is chosen as experimental pipeline samples. DN-250 was used in the FEM.

Table 3 Normal Pipe Size of DN-150

NPS	DN	Outer Diameter [in (mm)]	Wall thickness [in (mm)]											
			Sch. 5	Sch. 10s/10	Sch. 20	Sch. 30	Sch. 40s/40 /STD	Sch. 60	Sch. 80s/80 /XS	Sch. 100	Sch. 120	Sch. 140	Sch. 160	XXS[7]
6	150	6.625(168.28)	0.109 (2.769)	0.134 (3.404)	—	—	0.280 (7.112)	—	0.432 (10.973)	—	0.562 (14.275)	—	0.719 (18.263)	0.864 (21.946)

Table 4 Normal Pipe Size of DN-250

NPS	DN	OD [in (mm)]	Wall thickness [in (mm)]				
			Sch. 5s	Sch. 10	Sch. 20	Sch. 30	Sch. Std./40S
10	250	10.75 (273.05)	0.134 (3.404)	0.165 (4.191)	0.250 (6.350)	0.307 (7.798)	0.365 (9.271)

c) Epoxy: The Clear Casting and Coating Epoxy Resin - 16 Ounce (473ml) from Amazon.com (Figure 12) will be purchased as epoxy.

Figure 12 Epoxy coating product

With the experiment designed and materials purchased, in next quarter, we will test the survivability of the sensor array during the passing of a cleaning pig in lab.

2.3 Student Advising and Outreach

2.3.1 Student Advising:

During this quarter, two graduate students (Shuomang Shi, Ph. D. student, and Hafiz Usman Ahmed, Masters student) were hired to work on this project. The two graduate students worked on this project during Quarter 3 and they will continue work on this project next quarter. In addition, one graduate student from chemistry department, Wei Xu, dropped from his graduate study plan and left this project. To further continue the development of the chemical sensors, one new graduate student was recruited and will start working on this project at the end of July. Undergraduate research assistant did not work in summer and will come back in August 2019 to continue working on this project.

2.3.2 Outreach Activities:

In this quarter, as a part of NDSU NATURE summer camp, a lab tour was given to Native American high school students to give them opportunities to explore pipeline related research. Eight Native American high school students participated to this summer camp. Figure 13 show a photo taken during the outreach event.

Figure 13 Outreach to Native American students

2.4 Future Work

In the fourth quarter, there will be four objectives:

1) Task 2.1: Find an appropriate polymer matrix to dope the chemical sensor molecules for coating thin films on the steel substrate (Resume from Q2);

2) Task 2.2: Update FEM models in Quarter 2 based on the polymer selection in Task 2.1 and perform parametric analysis using FEM analysis on sensor aspect ratio, multiple pig velocity, and material selection would be considered to advise the sensor casting (Resume from Q2);

3) Task 2.2: Simulate survivability of the sensors in oil/gas environments with flow considered using appropriate tools;

4) Task 2.2: Experimentally test the survivability of the sensors with consideration of cleaning pigs passing by.

References:

Abdolkarimi, V. and Mohammadikhah, R., (2013). CFD Modeling of Particulates Erosive Effect on a Commercial Scale Pipeline Bend. *Hindawi Publishing Corporation ISRN Chemical Engineering*, 105912.

Ahmadvand, M., Najafi, A. F., and Shahidinejad, S. (2010). An experimental study and CFD analysis towards heat transfer and fluid flow characteristics of decaying swirl pipe flow generated by axial vanes, *Meccanica*, 45: 111-129.

Alias, A., Koto, J., Ahmed, Y.M., (2014). CFD simulation for stratified oil-water two phase flow in a horizontal pipe. *In: Proc. Ocean Mech. Aerosp. Sci. Eng*, 1, pp. 20–25.

Allievi, L. 1925. Theory of Water-hammer. *pography R. Garroni*.

Barten, W., Jasiulevicius, A., Manera, A., (2008). Analysis of the Capability of System Codes to Model Cavitation Water Hammers: Simulation of UMSICHT Hammer Experiments with TRACE and ELAPS. *Nuclear Engineering and Design*, 238(4): 1129-1145.

Chen, L., Duan, Y., Pu, W. and Zhao, C. (2009). CFD simulation of coal-water slurry flowing in horizontal pipelines. *Korean J. Chem. Eng*., 26(4), 1144-1154.

Dargahi, B. 2006. Experimental study and 3D numerical simulations for a free overflow spillway. *J. Hydraul. Eng. ASCE.* 132(9), 899-907.

Desamala, A. B., Dasamahapatra, A. K., and Mandal, T. K. (2014). Oil-Water Two-Phase Flow Characteristics in Horizontal Pipeline-A Comprehensive CFD Study. *International Journal of Chemical and Molecular Engineering*, Vol 8, No 4.

Dudlik, A., Schonfeld, S. B. H, and Schluter, S., (2002). Prevention of Water Hammer and Cavitational Hammer in Pipeline Systems. *Chemical Engineering&Technology*, 25(9): 888-890.

Ekambara, K., Sanders, R. S., Nandakumar, K., Masliyah, J. H. (2008). CFD simulation of bubbly two-phase flow in horizontal pipes. *Chemical Engineering Journal*, 144, 277-288.

Ekambara, K., Sanders, R. S., Nandakumar, K., Masliyah, J. H. (2009), Hydrodynamic Simulation of Horizontal Slurry Pipeline Flow Using ANSYS-CFX, *Ind. Eng. Chem. Res*, 48, 8159-8171.

Esmaeilzadeh, D. and Mowla, M. (2009). Mathematical modeling and simulation of pigging operation in gas and liquid pipelines, *J. Petrol. Sci. Eng.,* 69, 100–106.

Filion, Y. R., Karney, B. W. 2002. Extended-period analysis with a transient model. *Journal of Hydraulic Engineering-ASCE*, 128(6): 616-624.

Frank, T., Zwart, P.J., Krepper, E., Prasser, H.-M., and Lucas, D. (2008). Validation of CFD models for mono- and polydisperse air–water two-phase flows in pipes, *Nuclear Engineering and Design*, 238, 647-659.

Subhashini Ghorai, K.D.P. Nigam, (2006), CFD modeling of flow profiles and interfacial phenomena in two-phase flow in pipes, *Chemical Engineering and Processing*, 45, 55-65.

Ghidaoui, M. S. (2001). Fundamental Theory of Water Hammer, *Special Issue of the Urban Water J*. 1(2), pp. 71–83.

Ghidaoui, M. S. and Kolyshkin, A. A. (2001). Stability analysis of velocity profiles in water hammer flows. *J. Hydraul. Eng. ASCE*. 127(6)499–512.

Ghidaoui, M. S., Mansour, G. S., and Zhao, M. 2002. Applicability of quasi-steady and axisymmetric turbulence models in water hammer. *J. Hydraul. Eng. ASCE.* 128(10), 917-924.

Herra´n-Gonza´lez, A., De La Cruz, J. M., De Andre´s-Toro, B., and Risco-Martı´n, J. L. (2009). Modeling and simulation of a gas distribution pipeline network, *Applied Mathematical Modelling*, 33, 1584-1600.

Hu, H., and Cheng, Y. F. (2016). Modeling by computational fluid dynamics simulation of pipeline corrosion in CO_2-containing oil-water two phase flow. *Journal of Petroleum Science and Engineering*, 146, 134-141.

Jayakumar, J. S., Mahajani, S. M., Mandal, J. C., Iyer, K. N., and Vijayan, P. K. (2010). CFD analysis of single-phase flows inside helically coiled tubes, *Computers and Chemical Engineering*, 34, 430-446.

Joukowski, N. (1904). Water hammer. Proceedings of the Ameican Water Works Association, 341-424.

Kaushal, D. R., Thinglas, T., Tomita, Y., Kuchii, S., and Tsukamoto, H. (2012). CFD modeling for pipeline flow of fine particles at high concentration. *International Journal of Multiphase Flow*, 43, 85–100.

Muhlbauer, W. K. (2004). Pipeline Risk Management Manual. *Gulf Professional Publishing*.

Nieckele, A.O., Braga, A.M.B., and Azevedo, L.F.A. (2001). Transient pig motion through nonisothermal gas and liquid pipelines, *J. Energy Resour. Technol. ASME* 123 (4), 611–618.

Nikpour, M. R., Nazemi, A. H., and Dalir, A. H., (2014). Experimental and Numerical Simulation of Water

Hammer. *Arabian Journal for Science and Engineering,* 39(4): 2669-2675.

Ruprecht, A., and Helmrich, T. (2003). Simulation of the water hammer in a hydro power plant caused by draft tube surge. *Proc., 4th ASME_JSME Joint Fluids Engineering Conf., ASME, New York,* 2811–2816.

Saikia, M. D., Sarma, A. K. (2006). Numerical modeling of water hammer with variable friction factor. *J. Eng. Appl. Sci.* 1(4), 35-40.

Solghar, A. A., and Davoudian, M. (2012). Analysis of transient Pig motion in natural gas pipeline, *Mech. Ind.* 13, 293–300.

Streeter, V. L. and Wylie, E. B. (1998). Fluid Mechanics (International 9th Revised ed.), *McGraw-Hill Higher Education*.

Taha T. and Cui, Z. F. (2006). CFD modelling of slug flow in vertical tubes. *Chemical Engineering Science*, 61, 676-687.

Thorley, A. R. D. Fluid Transients in Pipelines (2nd ed.)*, Professional Engineering Publishing*, ISBN 0-79180210-8.

Wang, D. and Zhu, X. X. (2015). Comparison of linear and nonlinear simulations of bidirectional pig contact forces in gas pipelines. *Gas. Sci. Eng.* 27, 151e157

Wylie, E. B. and Streeter, V. L. (1984). Fluid Transients, FEB Press, Ann Arbor.

Wylie, E. B., Streeter, V. L., and Suo, L. (1993). Fluid Transient in Systems, Prentice-Hall, Englewood Cliffs.

Wood, D. J. (2005). Water hammer analysis-essential and easy (and efficient). *J. Environ. Eng. ASCE.* 131(8), 1123-1131.

Wood, D. J., Lindireddy, S., Boulos, P. F., Karney, B., and Mcpherson, D. L. (2005). Numerical methods for modeling transient flow in distribution systems. *J. Am. Water Works Assoc.* 97(7), 104–115.

Wu, D., Yang, S., Wu, P., and Wang, L. (2015). MOC-CFD Coupled Approach for the Analysis of the Fluid Dynamic Interaction between Water Hammer and Pump. *Journal of Hydraulic Engineering, ASCE*, ISSN 0733-9429/06015003(8).

Wu, D., Wu, P., Li, Z., and Wang, L. (2010). The transient flow in a centrifugal pump during the discharge valve rapid opening process. *Nucl. Eng. Des.,* 240(12), 4061-4068.

Zhang, H., Zhang, S., and Liu, S. (2015). Measurement and analysis of friction and dynamic characteristics of PIG's sealing disc passing through girth weld in oil and gas pipeline, *Measurement,* 64, 112–122.

Zhao, M., Ghidaoui, M. (2004). Godunov-type solutions for water hammer flows. *J. Hydraul. Eng. ASCE*, 130(4), 341-348.

Zhu, X. X., Zhang, S. M., Tan, G. B., Wang, D. G., Wang, W. M. (2014). Experimental study on dynamics of rotatable bypass-valve in speed control pig in gas pipeline. *Measurement,* 47, 686e692.

Zhu, X., Zhang, S., Li, X., Wang, D., Yu, D. (2015). Numerical simulation of contact force on bi-directional pig in gas pipeline: at the early stage of pigging. *J. Nat. Gas. Sci. Eng.* 23, 127e138.